Final Report

NASA Grant NNG05GJ23G

Refinement of Plasma Measurements from the Galileo Mission to Jupiter

May 15, 2005 – September 30, 2009

Principal Investigator:

Dr. William R. Paterson
Center for Atmospheric Sciences
Hampton University
Hampton, Virginia, 23668

1.0 Summary

The purpose of this project has been to produce useful scientific parameters to characterize the plasma environment observed with the plasma analyzers (PLS) on board the Galileo spacecraft. The parameters include the number densities, bulk-flow velocity vectors, and temperatures of the heavy-ion component of the plasmas. The heavy ions dominate the plasmas of the Jupiter system, and these parameters are extremely useful for analyses of plasma dynamics and processes of plasma production and loss. To ensure quality of the data products, several specific objectives have been met. These include: (i) Verification of calibration factors for the ion sensors; (ii) development of algorithms for systematic computation of moments accounting for several important quality factors related to limitations of the instrumentation and complications associated with Jupiter's plasma environment; and (iii) development of methods for quantitative estimation of uncertainties and errors. At this time, the computational methods have been developed for computing parameters and evaluating errors and uncertainties. Parameters have been delivered to the PDS covering all RTS (Real-Time Science) measurements to a radial distance 30 R_J (Jupiter Radii). These observations, which span a combined 129 days, were acquired during 31 of Galileo's 34 orbits at Jupiter. Plasma parameters from REC (recorded data) intervals are being processed for delivery to the PDS using the same methodology. Although the chief purpose of the project has been development of a data set, evaluation of those data requires consideration of scientific context, and results have been discussed at several conferences, which are noted in section 4.0. The remainder of this report documents the methods of analysis developed during the course of the project.

2.0 Instrumentation

The plasma instrumentation for the Galileo mission carried the designation PLS as did the plasma instrumentation for the prior Voyager missions. However, it differed considerably in design. The PLS has been described in detail by Frank et al., [1992]. The content of that paper is also available through the PDS PPI node. Some details of design and operation are reviewed here to provide context for discussion of the processing of data for the PDS.

The PLS was designed to measure electrically charged particles, both electrons and positively charged ions, with energies in the range of about 1 eV to ~ 50 keV. The particles in this range are frequently referred to as the thermal plasma, to distinguish them from the energetic charged particles at higher energies which were observed with separate instrumentation. The PLS was designed to provide coverage and resolution of particle energies and directions sufficient for characterizing the ion and electron velocity distributions. Those distributions can provide direct evidence of physical processes affecting the particles. Plasmas are quite often treated with a fluid, or multi-fluid approach, and if the velocity distributions are well measured, then it is also possible to compute fluid parameters for the different components of the plasma. These parameters include the number density, bulk flow velocity, pressure, and temperature, all of which can be different for the separate ion components and for the electrons.

For the Galileo mission, the PLS was mounted on a boom on the spinning section of the Galileo spacecraft. Charged particles entering the aperture on the entrance side of the deflection plates were selected according to their directions and their energies. Energy selection was accomplished by application of a bias voltage to one of the deflection plates. There were 64 possible voltage steps. Detection was accomplished when particles entered one of the spiraltron sensors on the exit side of the plates. Each sensor had its own field of view. There were 7 sensors for electrons and 7 matching sensors for positively charged ions with fields of view arranged to provide near complete coverage of the sky during the course of spacecraft rotation. There were in fact, two essentially independent sets analyzers, with their own deflection plates, sensors, and power supplies. The fields of view of the sensors of the two analyzers were complementary, though, and to achieve the best resolution and coverage of directions, the measurements are combined. The fields of view of the ion sensors are illustrated in Figure 1. The electron fields of view are similar. The sensors labeled a 1, 3, 5, and 7 were part of the A analyzer, while sensors 2, 4, and 6 belonged to the B analyzer. Additionally, there were three ion sensors that employed magnetic deflection to discriminate ions with different M/Q (mass per electronic charge). These mass spectrometers proved most often to be ineffective for routine identification of mass because they provided poor coverage of the sky, and because the signal to noise ratio in the Jupiter system was low, due to high rates of penetrating radiation. For that reason, mass-resolved ion data are not provided in this delivery of parameters to the PDS.

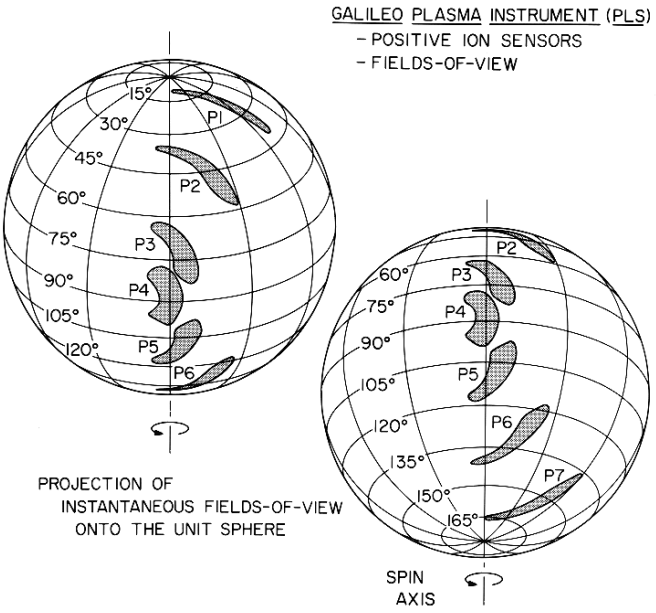

Figure 1. Fields of view of the 7 ion sensors of the Galileo PLS. Those of the electrons sensors are similar. This figure is adapted from Frank et al., [1992], but with corrected direction for the spin axis and sense of rotation.

2.1 Modes of Operation

During the Jupiter tour, the PLS operated in several different modes. Measurements at a pre-programmed subset of the possible energy steps were taken in evenly spaced rotation sectors. Sectoring was synched to the attitude control system, and thus was insensitive to changes in the rotation period. Measurements of ions and electrons of the same energy were simultaneous. To obtain greater resolution of energies, directions, and time, some data were recorded on the spacecraft tape recorder, and then replayed at a rate commensurate with the available telemetry rate, which was 10's of bits/second. The tape recorder capabilities were such that recordings were limited to durations of about 1 hour, or less, and were reserved for high priority time intervals, for example near encounters with the Galilean moons.

2.1.1 REC Modes The recorded modes that are used to compute parameters for the PDS took measurements in 12 different energy steps in each of 8 evenly spaced 45^o rotation sectors during a single spacecraft rotation. Accumulation time at each step was 0.15 second. A complete measurement cycle required a sequence of 6 rotations. Instrument operation during those rotations is summarized in Table 1. An initial rotation, designated Mode 19, utilized every 4th energy step from 13 – 61. Samples were taken by each of the 7 ion sensors in each of the 8 rotation sectors during Mode 19, and during subsequent Modes 20, 22, and 23. The next subsequent rotation (Mode 20) used every 4th step from 15 – 63, so that it covered roughly the same range of energies, but using interleaved energy steps. The 3rd rotation was dedicated to either mass spectrometry, or a special low energy mode not used in the present analysis. Hence, for present purposes, it can be considered "dead time". The 4th rotation (Mode 22) interleaved every 4th even step, from 12 – 60, and the 5th rotation, (Mode 23) interleaved every 4th step from 14 – 62. The 6th rotation was again dedicated to mass spectrometry or low energies, after which, the sequence repeated. Measurements of electrons and ions were simultaneous, and the above-described sequence applies equally to the electron sensors.

Table 1. PLS Recorded Data Modes for Ion Moments

	Rotation 1 Mode 19 *8 Sectors Sensors P1-P7 and E1-E7*		**Rotation 2 Mode 20** *8 sectors Sensors P1-P7 and E1-E7*		**Rotation 3** *Low E or Mass Mode*		**Rotation 4 Mode 22** *8 sectors Sensors P1-P7 and E1-E7*		**Rotation 5 Mode 23** *8 sectors Sensors P1-P7 and E1-E7*		**Rotation 6** *Low E or Mass Mode*	
SAMPLE	**STEP**	**eV**	**STEP**	**eV**			**STEP**	**eV**	**STEP**	**eV**		
1	13	10	15	15	-	-	12	9	14	12	-	-
2	17	21	19	29	-	-	16	17	18	25	-	-
3	21	41	23	57	-	-	20	34	22	48	-	-
4	25	80	27	112	-	-	24	67	26	95	-	-
5	29	157	31	220	-	-	28	132	30	186	-	-
6	33	310	35	461	-	-	32	251	34	379	-	-
7	37	695	39	970	-	-	36	549	38	842	-	-
8	41	1363	43	1962	-	-	40	1153	42	1647	-	-
9	45	2743	47	3843	-	-	44	2333	46	3221	-	-
10	49	5472	51	7777	-	-	48	4575	50	6533	-	-
11	53	10614	55	15189	-	-	52	8821	54	12810	-	-
12	57	21374	59	29829	-	-	56	17934	58	25254	-	-

This sampling scheme allows tradeoffs during the analysis that can be chosen to either maximize energy resolution, by using the full set of interleaved steps (4×13 = 52), or temporal resolution, by computing parameters for each individual rotation (13 steps), or pairs (26 steps). These options are available because each rotation covered a similar range of energies, though using a

different set of steps. In practice, it has most often proven optimal to combine Mode 19 and 20 to compute a set of parameters, and combine 22 and 23 to compute a set of parameters. This provides moments with a repetition rate of 3 spins, or about 1 minute, and with resolution of energy that is about one half of the best available resolution, and sufficient for characterizing the velocity distributions. Plasma parameters for the PDS are being computed using this scheme.

2.1.2 RTS Modes Because of the limitations on bit rate, and on use of the tape recorder, surveys of the Jupiter system were conducted using sampling schemes that made efficient use of the available telemetry. These data were not recorded onto the spacecraft tape recorder. They were buffered by the instrument processor for a short period of time, until they could be inserted into the telemetry stream for broadcast using the low-gain antenna at the available bit rate. Resolution of energies, directions, and time were reduced, but the data are adequate for many studies and are of considerable value because they provide the greatest available coverage of locations, and they provide near continuous coverage over long time intervals; of order weeks or months. Two different sets of RTS modes were used, designated RTS0 and RTS4. The RTS0 mode required less telemetry, and was used more frequently.

2.1.2.1 RTS0 The instrument operational sequence during RTS0 is summarized in Table 2. For RTS0, the rotation is divided into 4 equal 90^{o} sectors. The first rotation (Mode 166) sampled the lower range of ion energies for the A analyzer (detectors P1, P3, P5, P7) from step 11 to step 35, utilizing every 4^{th} step, with an accumulation time of 0.5 s. The data were buffered, and inserted into the telemetry stream. The amount of time required to clear the buffer was variable; dependent on the available bit rate. The next mode (Mode 167) did not begin until the buffer was cleared, which generally required multiple rotations. That mode covered the upper range of ion energies for the A analyzer, which included every 4^{th} step from 39 to 63. After those data have been read out, the next mode (Mode 198) sampled the lower ion energies for the B analyzer sensors (P2, P4, P6). Again, the data buffer would be cleared, and then, the final mode (Mode 199) completed the cycle by measuring the upper energies for the B analyzer. Because dead time between modes was variable, the amount of time required to complete a cycle was variable. The average duration of the RTS modes provided to the PDS was 9 minutes, and the minimum was 1.5 minutes. If the duration exceeded 30 minutes, parameters are not included in the PDS data set. Temporal aliasing is likely to be an important source of error for these observations. The magnitude of that error is difficult to estimate, but common sense would dictate that any scientific conclusion based on a single measurement probably is not robust.

Table 2. PLS Real-Time Mode RTS0

	Mode 166 *4 Sectors P1, P3 ,P5, P7*		⇔ Telemetry	Mode 167 *4 Sectors P1, P3 ,P5, P7*		⇔ Telemetry	Mode 198 *4 Sectors P2, P4, P6*		⇔ Telemetry	Mode 199 *4 Sectors P2, P4, P6*		⇔ Telemetry
SAMPLE	STEP	eV		STEP	eV		STEP	eV		STEP	eV	
1	11	7		39	970		11	7		39	970	
2	15	15		43	1962		15	15		43	1962	
3	19	29		47	3843		19	29		47	3843	
4	23	57		51	7777		23	57		51	7777	
5	27	112		55	15189		27	112		55	15189	
6	31	220		59	29829		31	220		59	29829	
7	35	461		63	52704		35	461		63	52704	

2.1.2.4 RTS4 Instrument operation during RTS4 was similar to RTS0 with the following exceptions. First, there were 8 rotational sectors rather than 4, so angular coverage and resolution were similar to the REC modes. Second, the energy range was divided into two sets of 8 steps each, by sampling every 3rd step, from 18 to 63. This sequence is illustrated in Table 3. The mode numbers (166, 167, 198, 199 for ions) remained the same. Because RTS4 required higher data rates, RTS0 was used more frequently. A summary of RTS coverage provided by the PDS data is given in Table 4.

Table 3. PLS Real-Time Mode RTS4

	Mode 166 *8 Sectors* *P1, P3 ,P5, P7*		⇔	Mode 167 *8 Sectors* *P1, P3 ,P5, P7*		⇔	Mode 198 *8 Sectors* *P2, P4, P6*		⇔	Mode 199 *8 Sectors* *P2, P4, P6*		⇔
SAMPLE	STEP	eV	Telemetry	STEP	eV	Telemetry	STEP	eV	Telemetry	STEP	eV	Telemetry
1	18	25		42	1647		18	25		42	1647	
2	21	41		45	2743		21	41		45	2743	
3	24	67		48	4575		24	67		48	4575	
4	27	112		51	7777		27	112		51	7777	
5	30	186		54	12810		30	186		54	12810	
6	33	310		57	21374		33	310		57	21374	
7	36	549		60	34770		36	549		60	34770	
8	39	970		63	52704		39	970		63	52704	

Both RTS0 and RTS4 differed from REC modes in that electrons and ions were sampled during different rotations. The electron modes (168, 169, 200, 201) were identical to the ion modes in number of sectors, and in choice of steps. However, electron samples and ion samples were asynchronous. The electron modes were interleaved with the ion modes, and thus contributed to the delay between sampling of lower/upper ion energies and between the A/B analyzers. For simplicity, this additional delay is incorporated into the dead-time column labeled as "Telemetry" in Tables 2 and 3.

3.0 Plasma Parameters

The parameters are to be incorporated in the Planetary Plasma Interaction node (PPI) of NASA's Planetary Data System (PDS). Introduction of these parameters is a significant advancement over the current state of the data holdings. The data that have been available include a complete record of the measured counting rates from the various sensors of the PLS, along with calibration factors required for deriving physical quantities, including derived parameters such as those discussed here. However, use of those data requires detailed knowledge of the operation of the PLS. Additionally, there are necessary approximations and simplifications to be made during the course of the analysis and development of algorithms, as is discussed below. These stem from the limitations of the instrumentation and the operating modes. As part of this project, errors and uncertainties in measurements from the PLS have been quantitatively assessed for the first time. That assessment required development of simulations of instrument response. The simulations are used to correct for systematic errors associated with the limitations of the measurements, and 1-sigma level uncertainties are being provided to the PDS as a guide to reliability of the measurements. Those uncertainties include the statistical variation associated with counting, uncertainty due to possible variations in ion composition, and inherent uncertainties associated

with finite resolution and coverage of energies and directions. This latter contribution is determined through a simulation described below.

Table 4. RTS Coverage for R < 30 R_J

Orbit	Start	End	Samples	
			RTS0	RTS4
1	1996-177/17:00	1996-182/07:06	277	0
2	1996-249/04:26	1996-253/19:54	283	0
3	1996-309/04:42	1996-313/22:59	283	0
4	1996-351/18:00	1996-356/14:45	242	0
6	1997-049/10:59	1997-054/06:49	257	27
7	1997-092/02:25	1997-096/20:55	220	82
8	1997-126/08:42	1997-130/19:15	290	160
9	1997-176/04:46	1997-180/19:44	286	292
10	1997-259/17:33	1997-264/07:57	228	167
11	1997-308/15:41	1997-313/11:00	215	97
12	1997-349/08:14	1997-350/19:45	76	0
14	1998-087/13:14	1998-090/01:39	128	0
15	1998-150/21:13	1998-152/19:21	99	0
16	1998-201/05:08	1998-201/17:15	28	24
17	1998-268/04:43	1998-270/01:12	124	40
18	1998-325/12:10	1998-328/13:23	71	0
19	1999-031/02:19	1999-032/01:13	38	0
20	1999-122/17:08	1999-125/20:04	144	0
21	1999-181/00:15	1999-184/10:25	239	0
22	1999-223/14:05	1999-226/10:09	264	0
23	1999-256/21:44	1999-260/03:02	232	22
24	1999-283/04:07	1999-285/05:44	140	0
25	1999-329/04:55	1999-329/19:50	72	0
26	2000-001/23:31	2000-005/01:20	346	0
27	2000-052/04:36	2000-054/17:23	131	0
28	2000-140/04:57	2000-144/03:49	215	0
29	2000-362/01:39	2000-366/05:46	227	0
30	2001-143/13:15	2001-145/19:34	58	0
31	2001-217/05:49	2001-219/15:09	108	0
32	2001-287/02:13	2001-291/00:48	186	0
33	2002-015/15:57	2002-019/14:26	333	0

In principle, it can be a straightforward exercise to derive plasma parameters from the plasma measurements. The PLS measured particle flux for electrons and for positively charged ions as functions of energy and angle. If the plasma is comprised of electrons and a single ionic mass/charge species, and the flux is measured with adequate coverage and resolution of both particle energy and direction, then parameters are computed as a summation over velocity of the intensities, with appropriate weighting functions, which include factors of velocity raised to the power 0, 1, 2, etc. This is done separately for the electrons, and for the ions. In the case of a single positive or negative species, particle velocity can be derived directly from the measured energies and directions of the particles. The measured intensities are directly proportional to the phase-space densities of the particles, commonly known as the particle velocity distribution, and

the summations are moments of that distribution. Number density is the zero-order moment. The bulk-flow velocity is the first order moment, pressure the second order moment, and the temperature can be derived from the pressure and the density.

In the Jupiter system, there are major complicating factors which make this procedure approximate, at best. Simply put, the measurement constraints noted above are violated. There are multiple ion M/q species, which are only partially separable, and particle energies and directions may be poorly covered and/or poorly resolved. This latter complication is especially true for instrument operation during real-time survey (RTS) intervals. The RTS data was transmitted directly to Earth at low bit rates using the low-gain antenna. As discussed in a previous section, sampling schemes were decimated to meet telemetry constraints. This allowed for successful completion of Galileo Mission objectives, though with some degradation in the quality of the observations.

3.1 Heavy Ion Plasma Parameters

The ion plasma in the Jupiter system is not made up of a single M/Q ion species. The major species are heavy ions originating from the cloud of neutral gas associated with Io. These include various charge states of atomic oxygen and sulfur (O^+, O^{2+}, O^{3+}, S^+, $S^{2+)}$, and in the near vicinity of Io there may be significant densities of ionized compounds of oxygen and sulfur, e.g. SO_2^+. Water-group ions are contributed by the icy moons at larger radial distances, and protons are present due to breakup of water-group molecules, but also may originate from the solar wind and from the Jovian atmosphere. The Voyager PLS had sufficient energy resolution that it was able to identify major ion species when the plasma was cold. For that purpose, cold means that the thermal speeds for the various ion distributions are small compared to the common velocity of bulk flow imposed by Jupiter's rotation. If such is the case, then the ion energy distributions, which have common velocity, resolve to individual peaks. On that basis, it is known that the dominant species has M/Q = 16 AMU/e, which can be either singly ionized atomic oxygen, or doubly ionized sulfur atoms. Although Galileo could not routinely determine M/Q, the mass-resolved spectra that are available support the Voyager determination.

Because computation of the plasma parameters requires summation over particle speeds, not energies, and because the phase space distribution is related to the measured ion flux by a factor $(M/Q)^2$, exact computation of plasma moments requires separation of the different M/Q ion species. The ion sensors P1 – P7 could easily separate light ions (protons, possibly H_2^+) from heavy ions, but did not have sufficient resolution of energy to provide separation of the various different heavy ions from one another. An exception occurred in the very cold plasma torus inside the orbit of Io recorded during orbit A34, but those data suffer from other complications, related to the low temperature and very high mach number for the flow there.

To provide approximate heavy-ion parameters, the following procedure is used for computation of moments. First, the protons are effectively eliminated by setting a lower cutoff energy which is equal to 4 times the energy of a corotating ion, which is also ½ the energy for corotating O^{2+}. Second, the heavy ions are then treated as a single M/Q species. Because MQ = 16 AMU/e is predominant, that value is selected for the computation. The moments are then computed as appropriately weighted summations over energy and direction. The range of errors caused by variation of composition is discussed in detail in the following section. As a refinement, the

computation is iterated one time. After the initial computation of the parameters, which include temperature, the temperature is used to limit the range of summation to directions and energies that fall within 1 kT of a centroid corresponding to the bulk flow velocity. The purpose of the iteration is to eliminate samples that may be due to statistical fluctuation of penetrating background radiation escaping the background subtraction, and to mitigate artificially high temperatures due to the presence of trace ions with high M/Q.

3.2 Uncertainties and errors in heavy ion parameters

Uncertainties and systematic errors in the heavy ion parameters are found to be strongly dependent on the mach number of the flow and the angle of attack of the beam with respect to the spin axis of the spacecraft. Errors due to variation of the composition of the heavy ions are found to be acceptable for many purposes, so long as the composition does not differ greatly from that determined with Voyager.

3.2.1 Errors associated with composition Fortunately, the computed densities and bulk flow velocities are not extremely sensitive to the composition. For a single ion species, the density computed from a given flux is proportional to the assumed value of $(M/Q)^{1/2}$, and velocity is proportional to $(Q/M)^{1/2}$. For example, if densities are computed with the assumption that M/Q is 16, when it is actually comprised entirely of M/Q = 8, then the computed density is higher than the actual by a factor of $2^{1/2}$ =1.4, and the computed speed is low by the inverse factor 0.7. If the actual plasma is a mix of M/Q = 8 and M/Q =16, then the errors are less. Addition of modest densities (~10%) of M/Q = 32 do not significantly affect the parameters computed using the procedure described above. Likewise, M/Q = 10.66 (S^{3+}) does not greatly affect the accuracy of densities and flow speeds, which are more significantly affected by other factors. Temperature is generally a more complicated quantity. For a single species it is proportional to the assumed value of M/Q. If there are multiple species with comparable densities, then the energy distribution spreads in the direction of flow, and that can lead to an artificially higher temperature. However, if one species is dominant, then that effect is mitigated, and the perpendicular component of temperature is not affected, though perpendicular temperatures of different species may be different.

3.2.2 Errors associated with penetrating radiation In addition to those particles entering through the aperture of the PLS with energies in the range of acceptance, the sensors also count in response to energetic penetrating radiation, and there is a substantial background at Jupiter that often greatly exceeds the signal of the thermal plasma. This background is the principal reason why the decline in response of the electron sensors was not immediately evident. Computation of parameters requires subtraction of that background. Fortunately, the response to thermal ions is generally limited to a particular range of directions and energies. This is due to the relatively high mach number of the flow, which is a consequence of Jupiter's rapid rotation. For moments delivered to the PDS, background rates for ions are computed by taking an average response in the lowest energy steps, and an average response in the highest steps. Whichever rate is lower is taken as the background rate, which is then subtracted from the signal. After subtraction, samples are included in computation of parameters only if they are two-sigma or more above the background, where sigma is the uncertainty in the count rate based on Poisson statistics.

3.2.3 Errors associated with high mach number The high-mach flow of the ions is also a source of uncertainty. Because of the geometry of the sensors, systematic errors in measurements increase with increasing mach number, and they are most severe for beams directed at 90^o relative to the spin axis, and least severe for beams near 0^o and 180^o. The detectors have finite resolution of direction. Inherent resolution of azimuth is $\sim 5^o$, and resolution of polar angle is larger, $\sim 20^o$. If the mach number is especially high, ~5 and more, then the angular width of the observed beam may be less than the resolution of the detector. Additionally, the spread in energy may be comparable to or smaller than the gaps between the energy bands. Resolution of energy $\Delta E/E \sim 0.1$ at each step, and the magnitude of the energy steps increases logarithmically. The energy bins are not contiguous, and in general not all bins are sampled when computing moments. Thus beams may fall into the gaps and be under-sampled. Also, measurements of a given energy are separated in azimuth by 45^o for the REC mode and RTS4, and by 90^o for RTS0. During the course of rotation through a given sector, energies increase sequentially. This coupling of energy sampling to rotation adds complexity to the analysis of high mach number beams. If beam intensity peaks in a localized part of a sector at an energy not matching the energy step in that part of the sector, then it is also under-sampled or missed. This effect is most pronounced for the equatorial sensor, P4, and much less important for beams near the spin axis, because directions separated by substantial azimuth angles are actually not widely separated in direction for the polar detectors. The spin axis of the spacecraft was pointed toward Earth for alignment of the low gain antenna, and thus it was approximately within Jupiter's equatorial plane and generally pointed toward the sun. As a consequence, corotating beams were nearly aligned with the spin axis when the spacecraft was near dawn or dusk, and near perpendicular when the spacecraft was near noon and midnight.

3.2.4 Quantitative estimation of combined uncertainties Because of the complexity of the sampling schemes and the geometry of the sensors, systematic errors as described above effectively translate to uncertainty. The magnitude of the likely error is quantitatively assessed through a simulation. With the exception of the Poisson statistic contribution, the errors are coupled and are best estimated with a simulation that treats masses, angle of attack, and mach number simultaneously. For the simulation, velocity distributions are modeled as Maxwell-Boltzmann distributions. The distributions are computed for ensembles of directions, bulk flow speeds, temperatures, and compositions. Those model distributions are then used as input for computation of simulated plasma moments using energy and directional bins identical to the actual instrument modes. The finite angular resolution of the sensors and variation of accepted particle energies across the sensor fields of view are accounted for using results from particle trajectory calculations. The range of possible output values for the computed densities, velocities, and temperatures for given set of input values is computed. That range of values is treated as an uncertainty. For the uncertainties provided with the PDS data, composition was taken to be a mix of M/Q = 8 and M/Q =16. The concentration of the lower M/Q ion was varied from 30% to 50%, and the heavier ion from 70% to 50%. Addition of 10% M/Q = 32 was investigated, and did not substantially change the simulation results.

As expected, the magnitude of the uncertainty increases with increasing mach number and increasing angle of attack for the beam relative to the spin axis. Results of simulations for the RTS modes are shown in Figures 2 and 3. Figure 2 shows systematic offsets and the 1-sigma range of measured values compared to the input values for density, temperature, and flow speed.

The first column, for example, shows the average output density <N> compared to the input value, N. The top panel is for angles of attack between 0^o and 40^o; the panel in the middle row for angles 40^o to 70^o, and the bottom row is for 70^o to 90^o. The abscissa in each panel indicates the mach number. For the smallest angles of attack, the moments calculation will compute densities that, on average, are larger than the actual by factors ranging from about 20% at mach 1 to 50% at mach 7, and the range of likely values increases with increasing mach number. For the largest angles of attack, the average computed densities are actually somewhat better, but the range of likely values is much larger. Overall, RTS4, shown in red, is both more accurate and more precise than RTS0, shown in blue. Figure 3 shows the speed, repeated from Figure 2, and also the range of uncertainty in direction. Polar angle is measured from the spin axis, and azimuth corresponds to rotation. Uncertainties in both angles grow with increasing mach number and angle of attack, but systematic offsets are generally small, ~10^o, or less.

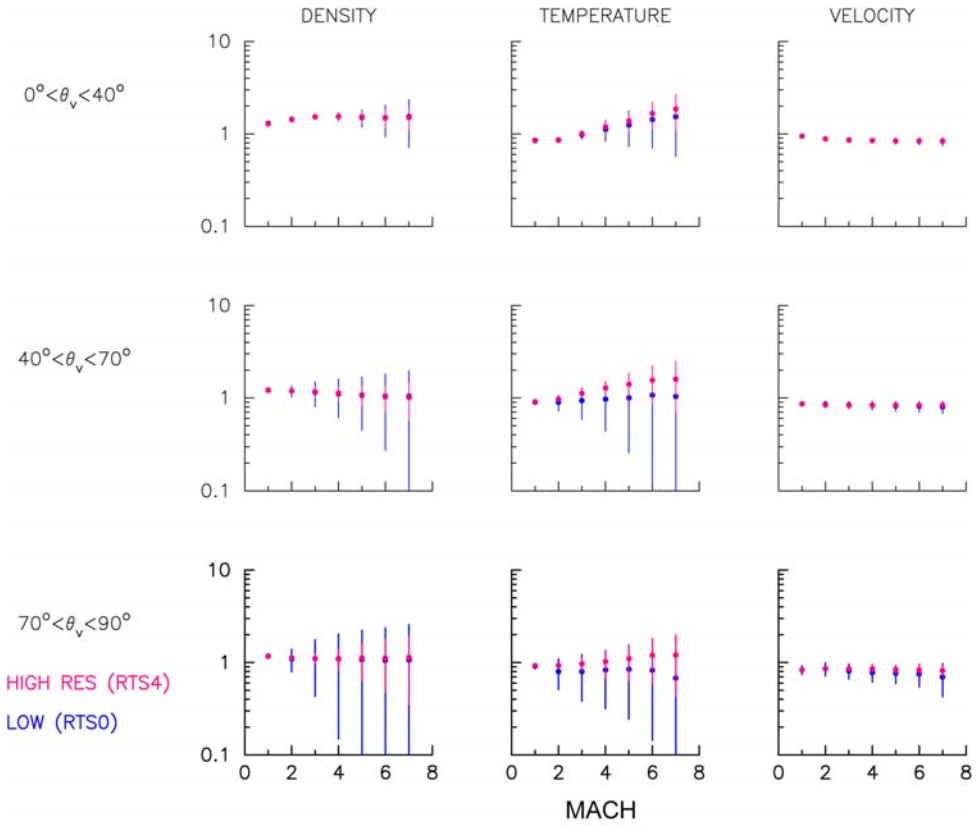

Figure 2. Simulated uncertainties for ion density, temperature, and speed for three different ranges of θ_v, which is the angle of attack for the incident flow vector with respect to the spin axis of the spacecraft. The uncertainties are symmetric with respect to the midplane, $\theta_v = 90^o$.

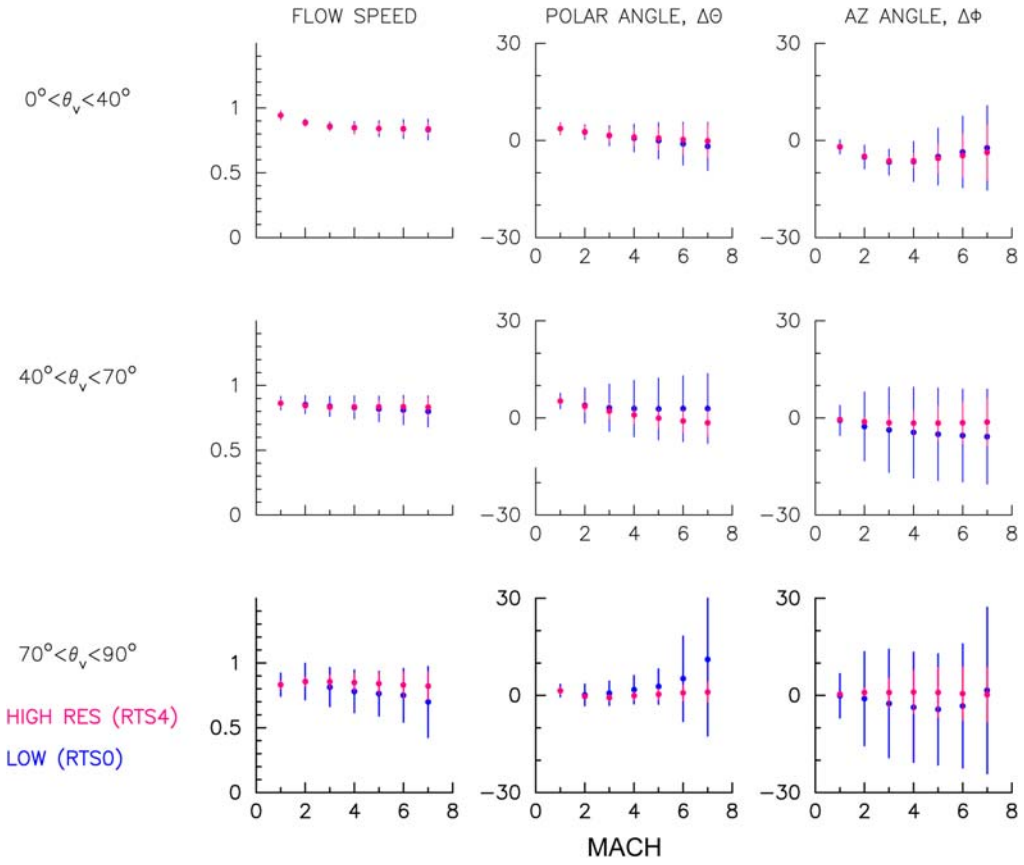

Figure 3. Continuation of Figure 2, showing ranges of uncertainty for the direction of flow, and for the speed, which is repeated from Figure 2, but on a linear scale.

For the parameters delivered to the PDS, the offsets of the average values are used as correction factors for the densities, speeds, and temperatures computed from the observed fluxes, and the range of uncertainty is combined with the counting statistics to produce an estimate of the overall uncertainty in the measurement due to those considerations described above. Parameters derived from RTS0 measurements during orbit 26 are shown in Figure 4, with correction factors applied and error bars indicated. If error bars are not visible, they are smaller than the dimension of the points.

3.2.5 Calibrations Initial in-flight calibration was performed during the first encounter of the spacecraft with Earth in December 1990. Ion sensor cross calibration and electron sensor cross calibration were accomplished in isotropic hot plasmas of the plasma sheet. The overall density calibration was set to match densities observed with IMP 8 in the magnetosheath, with Galileo situated downstream and IMP 8 upstream. Verification of the long term stability of the ion calibration is demonstrated through comparison with plasma wave emissions and cutoffs in the Jovian magnetosphere. The densities determined from plasma waves are total electron densities. The ion densities are approximately equal to the ion number density, with the approximation stemming from considerations discussed above. Ions with charge states 2 and 3 comprise some

fraction of the plasma, and it is typically assumed from known constraints on composition that electron density exceeds ion number density by a multiplicative factor ~1.5.

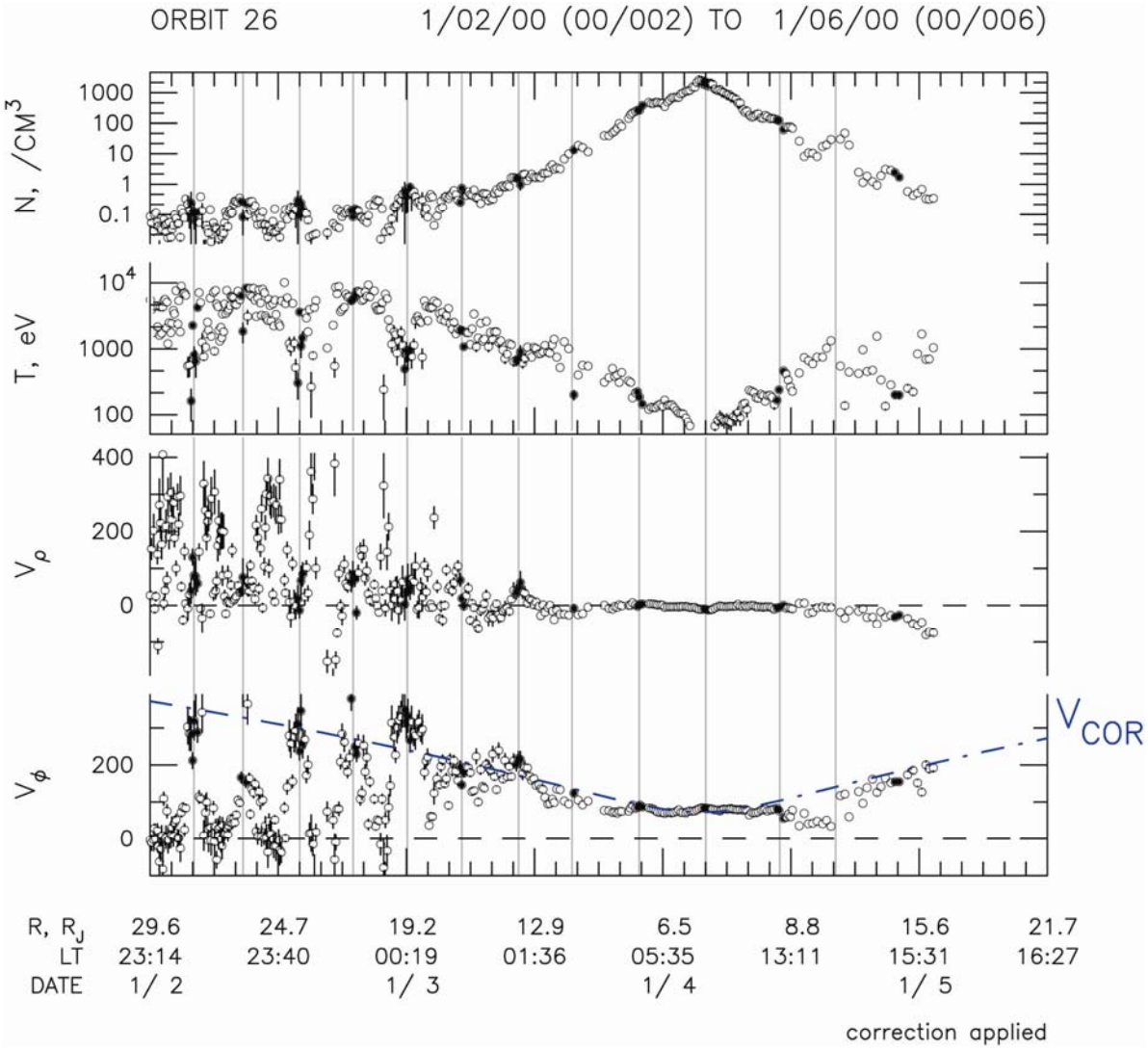

Figure 4. Heavy ion plasma parameters from the PLS during January 1 – January 4, 2000. These are derived from RTS0 measurements, as described in the text. Error bars are combined uncertainties from Poisson statistical fluctuations and from the range of systematic errors predicted by a simulation, and correction factors from the simulation have been applied. Vertical lines indicate crossings of the current sheet, as indicated by reversals of the radial component of the magnetic field. Black points are those within about 30 minutes of a crossing.

The overall good cross calibration of densities is demonstrated in Figure 5. Ion number densities computed for RTS measurements are used in combination with magnetic field measurements to predict the upper hybrid frequency, which depends most heavily on the charge density. At radial distances from Jupiter ~ 9 R_J, and less, there are typically emissions or cutoffs associated with the plasma frequency or the upper hybrid frequency that compare well with the independent predictions based on measured ion number density. At greater distances, emissions that may be

associated with electron densities are difficult to discern. For the latter part of the mission, perijove distance was reduced, and direct comparisons such as those given in 5 demonstrate that the methodology for determining densities, and the calibrations established at Earth are generally consistent with the observed plasma waves, especially given the uncertainties inherent to the plasma measurements, and other uncertainties in methodology.

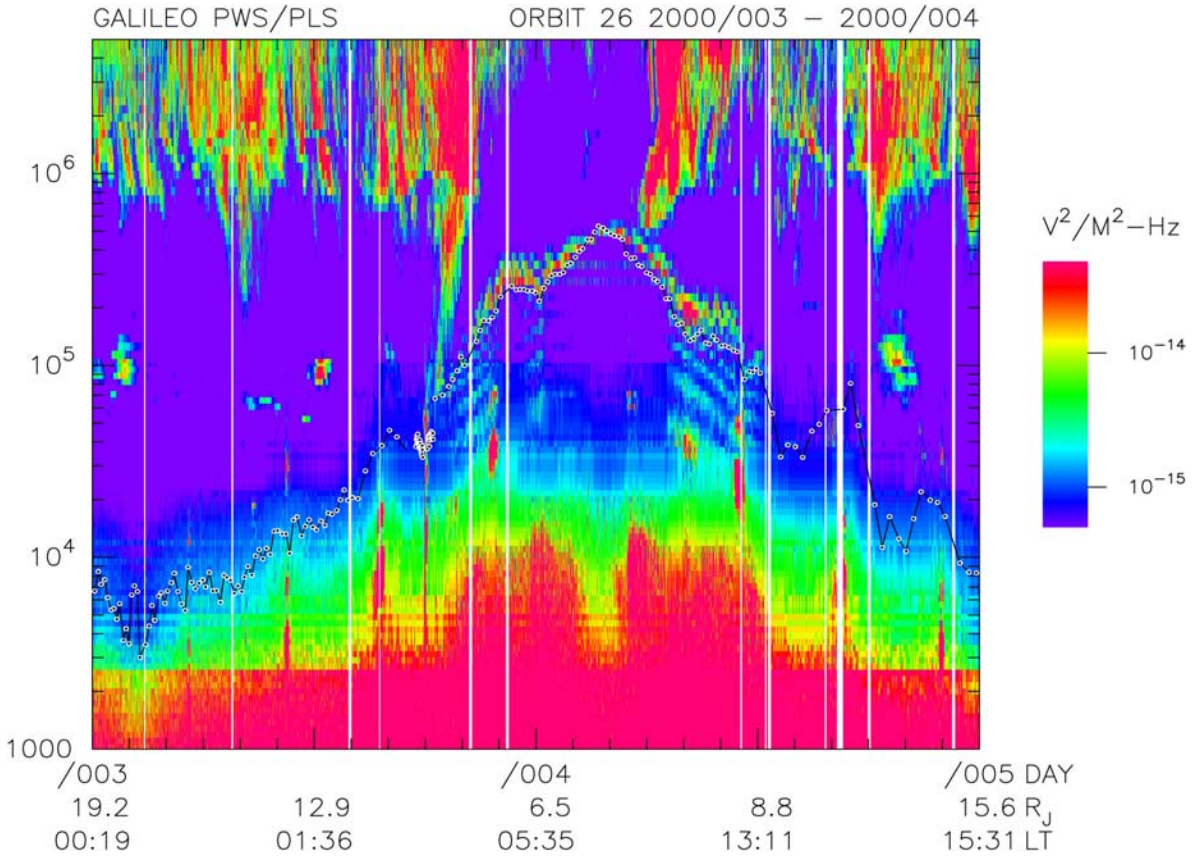

Figure 5. Plasma waves from the Galileo PWS near perijove during Orbit 26. Predicted emissions based on the PLS determination of heavy-ion number density are overlaid as a solid black line with measurements points indicated. The prediction is for the upper hybrid resonance, which depends on the electron density and the magnetic field strength. It depends most heavily on the electron density, which is equal to the ion number density to within a multiplicative factor ~1.5.

3.2 Electron Parameters

Following the Jupiter orbit insertion (JOI) on December 7, 1995, the electron sensors suffered degradation in their response to particles in the lower part of the PLS energy range. During the orbit insertion itself, as the spacecraft traversed the plasma torus, the sensors recorded the incident flux at all energies. Response was consistent with the calibration in the terrestrial plasma sheet. Evidence for this is the relatively good agreement between measured electron densities and ion densities, once the spacecraft potential had been taken into account. Prior to JOI periapsis, PLS operations were suspended, and sampling did not resume until day 175 of 1996. At that time, the electron sensors were no longer capable of detecting electrons with

energies less that about 100 eV. Below 100 eV, the sensors continued to count penetrating radiation, but there is evidence of the ambient thermal plasma. Over time, the threshold energy required to produce counts increased in an approximately linear fashion, and eventually was in the range of one to several keV. From Voyager, it is known that the bulk of the thermal electron distribution lies at energies several eV to several 10's of eV. Because of the sensor degradation, it is not possible to compute plasma parameters for the thermal electrons. A high energy tail was observed in the plasma torus and the magnetosphere. The cause of the sensor degradation may have been deposition of contaminants on the active surfaces within the channeltron sensors. The post-acceleration voltage for electrons was only ~10's of volts, and could not be adjusted to compensate for the keV threshold.

4.0 Presentations

Paterson, W. R., Ion Temperatures and Densities in Jupiter's Middle Magnetosphere and Consequences for Aurora, Magnetospheres of the Outer Planets, San Antonio, TX, June 2007.

Paterson, W. R., Properties of Ions in Jupiter's Magnetosphere, *Eos Trans. AGU, 88*(52), Fall Meet. Suppl., Abstract SM44A-05, December 2007.

Paterson, W. R., Plasma Flow in Juptier's Inner and Middle Magnetosphere, *Eos Trans. AGU, 89*(53), Fall Meet. Suppl., Abstract SM32A-06, December 2008.

Reference

Frank, L. A., K. L. Ackerson, J. A. Lee, M. R. English and G. L. Pickett, The Plasma Instrumentation for the Galileo Mission, Sp. Sci. Rev., 60, 283-307, 1992.